Journal of Applied Mathematics and Physics, 2024, 12, 3816-3826
https://www.scirp.org/journal/jamp
ISSN Online: 2327-4379
ISSN Print: 2327-4352

Dynamic Response of Tensile Membrane Structure under Coupling Effect of Wind and Rain

Weiju Song[1,2,3*], Heyuan Yang[3], Jie Chen[3]

[1]School of Civil Engineering, Tianjin University, Tianjin, China
[2]Huaheng Construction Group Co., Ltd., Ningbo, China
[3]School of Civil Engineering, Hebei University of Engineering, Handan, China
Email: *nimrodsong@126.com

How to cite this paper: Song, W.J., Yang, H.Y. and Chen, J. (2024) Dynamic Response of Tensile Membrane Structure under Coupling Effect of Wind and Rain. *Journal of Applied Mathematics and Physics*, **12**, 3816-3826.
https://doi.org/10.4236/jamp.2024.1211229

Received: November 1, 2024
Accepted: November 19, 2024
Published: November 22, 2024

Abstract

Because of the small stiffness and high flexibility, the tension membrane structure is easy to relax and damage or even destroy under the action of external load, which leads to the occurrence of engineering accidents. In this paper, the damped nonlinear vibration of tensioned membrane structure under the coupling action of wind and rain is approximately solved, considering the geometric nonlinearity of membrane surface deformation and the influence of air damping. Applying von Karman's large deflection theory and D'Alembert's principle, the governing equations are established for an analytical solution, and the experimental results are compared with the analytical results. The feasibility of this method is verified, which provides some theoretical reference for practical membrane structure engineering design and maintenance.

Keywords

Tension Membrane Structure, Wind and Rain Coupling Effect, Dynamic Response, Nonlinear Vibration

1. Introduction

The membrane material of the membrane structure is light in weight, small in stiffness, and low in natural frequency, so it is very sensitive to wind load and other loads (such as hail, rainstorm, etc.) and is prone to large deformation. Long-term load will also lead to relaxation and wrinkles in the membrane structure and then engineering accidents [1]-[3]. In recent decades, there have been many examples of membrane structures being damaged under wind load. On November

10, 2013, the famous landmark building in Sanya, Hainan, China—"Crown of Beauty" was lifted by a strong typhoon. On February 18, 2022, a storm hit the Isle of Wight in the United Kingdom, causing the roof membrane of the O2 Stadium in London (formerly known as the Millennium Dome) to be torn by the wind. The damage to the above building structures caused huge economic losses. However, it can be seen from the above engineering accident cases that when the membrane structure is destroyed, it is not only subject to wind load, but also accompanied by rainstorm load, and the influence of rainstorm load cannot be ignored.

The study of wind-rain coupling was mainly used for long-span bridge structures in the early days. In 1984, Hikami and Shiraishi [4] observed the Meikonishi Bridge in Japan, and found that the stay cables produced large and violent vibrations under the wind-rain coupling, and then began to study the wind-rain coupling phenomenon. In 2002, Blocken and Carmelie [5] carried out a numerical simulation of low-rise housing structures under the combined action of wind and rain, and considered the spatial distribution of instantaneous rainfall, wind-driven rain, and the influence of time factors; Sankaran [6] studied the pressure change of raindrops hitting the building wall, calculated the wind pressure distribution on the building surface and compared it with the results measured by wind tunnel test, and then used raindrops with different particle sizes to act on the building surface on the upper and top surfaces of the building. The results showed that when the wind speed was large, the impact of raindrops could not be ignored. According to the actual calculation of the relationship between wind speed and rain intensity, Choi [7] concluded that the maximum effect of wind-driving rain can exceed 20%.

In China, in 2007, Li Hongnan *et al.* [8] carried out a nonlinear time history analysis and solution of wind excitation and wind and rain joint excitation for transmission towers and transmission tower line systems, respectively, and drew the conclusion that the rain load in the design cannot be ignored; Chen Bowen *et al.* [9] applied CFD numerical simulation method to analyze the distribution law of wind and rain load on the windward wall of low-rise buildings, focusing on the influence of rain intensity, wind speed and roof structure on the structure. The analysis showed that the additional load caused by rainfall under extreme meteorological conditions could exceed 30% of the pure wind load. In 2014, Fu Xing *et al.* [10] gave an improved rain load calculation formula, obtained the time history curve of wind-driven rain load through numerical simulation, calculated the vibration frequency of transmission tower under wind-driven rain load, and compared it with the wind tunnel test results to verify the correctness of the theory; Wang Hui *et al.* (2014) [11] showed that the combined effect of wind and rain loads in extreme weather should be considered when designing engineering structures, especially cladding structures. In 2018, Cui Wenhui *et al.* [12] used the multiphase flow Euler-Euler model to establish a wind-rain load interaction model, considering factors such as the effect of raindrops on the wind field and the influence of wind-driven rain on the tensile membrane structure, and studied the

influence of changes in wind speed and rainfall on the surface wind pressure distribution of saddle-shaped membrane structure and the static response of the structure through numerical simulation. The results show that the effect of wind-driven rain load on membrane structure cannot be ignored. In 2018, Tian Li *et al.* [13] proposed a time history analysis method of rain velocity based on the equation method and program method and established a formula for calculating wind-driven rain load on this basis. In addition, Li Hongnan (2012) [14] and Gao Ganfeng *et al.* (2015 [15], 2016 [16]) also studied the dynamic response of glass curtain walls and large wind turbines under wind-driven rain load and obtained valuable conclusions. In 2021, Jiang Su [17] carried out numerical and experimental research on the dynamic response of saddle-shaped membrane structure under wind-driven rain load. In 2023, Pan Jierong *et al.* [18] studied the dynamic response and structural reliability of saddle-shaped membrane structures under wind-driven rain load through finite element numerical simulation and wind tunnel test.

Obviously, scholars have little research on the dynamic response of membrane structure, a flexible structure, under wind-driven rain load, and rarely focus on the analytical theoretical research of this problem. In this paper, the tension membrane structure commonly used in engineering is taken as the research object, and the damped nonlinear vibration of tension membrane structure under the coupling action of wind and rain is approximately solved. The governing equations are established for an analytical solution, and the research results will provide a theoretical basis for how to reasonably consider the increasing effect of wind and rain coupling on the dynamic response of membrane structure, improve the design and construction theory of membrane structure, and better guide the design and construction of membrane structure.

2. Coupling Effect of Wind and Rain

The aerodynamic force acting on the unit area of the projection surface of the membrane structure is

$$P_W = p_2 - p_1 \tag{1}$$

where, p_2 is the dynamic air pressure outside the membrane structure; p_1 is the air pressure inside the structure, which can be approximately equal to the air pressure p_∞ generated when the uniform flow field is not disturbed.

It is assumed that the incoming flow is a uniform and incompressible inviscid ideal fluid, which flows along the structure x direction at a velocity V and does non-rotational motion. The expression of the aerodynamic force acting on the surface of the streamlined structure is [19] [20]:

$$p_2 = -\frac{\rho_0}{2\pi}\left(-V\iint_{Ra}\frac{\left(V\frac{\partial z}{\partial y}+\frac{\partial w}{\partial t}\right)_{\substack{x=\xi\\y=\eta}}(y-\xi)}{\left(\sqrt{(x-\xi)^2+(y-\eta)^2}\right)^3}\mathrm{d}\xi\mathrm{d}\eta+\iint_{Ra}\frac{\left(V\frac{\partial^2 z}{\partial y\partial t}+\frac{\partial^2 z}{\partial t^2}\right)_{\substack{x=\xi\\y=\eta}}}{\sqrt{(x-\xi)^2+(y-\eta)^2}}\mathrm{d}\xi\mathrm{d}\eta\right)+p_\infty \tag{2}$$

where ξ and η are the position coordinates when the gas flow arches along the membrane surface, ρ_0 is the gas density, w is the displacement function of the membrane surface, and Z is the surface function of the membrane surface.

Substituting Equation (2) into Equation (1), then,

$$p_W = -\frac{\rho_0}{2\pi}\left(-V\iint_{Ra}\frac{\left(V\frac{\partial z}{\partial y}+\frac{\partial w}{\partial t}\right)_{\substack{x=\xi\\y=\eta}}(y-\xi)}{\left(\sqrt{(x-\xi)^2+(y-\eta)^2}\right)^3}\mathrm{d}\xi\mathrm{d}\eta + \iint_{Ra}\frac{\left(V\frac{\partial^2 z}{\partial y\partial t}+\frac{\partial^2 z}{\partial t^2}\right)_{\substack{x=\xi\\y=\eta}}}{\sqrt{(x-\xi)^2+(y-\eta)^2}}\mathrm{d}\xi\mathrm{d}\eta \right) \quad (3)$$

Regarding the rain load, according to Newton's second law, the load of a single raindrop in time Δt can be obtained as follows:

$$F(\Delta t) = \frac{1}{\Delta t}\int_0^{\Delta t} p(t)\mathrm{d}t = \frac{mv}{\Delta t} \quad (4)$$

where $p(t)$ is the impact force vector of a single raindrop, and m is the mass of the raindrop.

Assuming that the shape of the raindrop is a standard spherical shape, the action time of the raindrop is $\Delta t = d/2v$, and the mass of the raindrop is $m = \rho_w \pi d^3/6$, that is:

$$F(\Delta t) = \frac{\pi\rho_w d^2 v^2}{3} \quad (5)$$

Transforming the force of a single raindrop into a time-varying uniformly distributed load:

$$P_R = \frac{F(\Delta t)}{\pi d^2/4}\cdot\frac{1}{6}\pi d^3 n(D) \quad (6)$$

Substituting Equation (5) into Equation (6), then:

$$P_R = \frac{2}{9}\rho_w \pi d^3 n(D) v^2 \quad (7)$$

The wind-rain coupling model is formed by superimposing the aerodynamic model and rain load model. According to the aerodynamic model and rain load model, the expression of wind-rain coupling action can be obtained:

$$P = P_W + P_R \quad (8)$$

3. Dynamic Governing Equation of Membrane Structure under Wind and Rain Coupling Effect

Take the micro-cell *dx*, *dy* on the vibrating membrane, as shown in Figure 1 below. In the x direction, the unit can be regarded as composed of countless chord elements with a length of *dx* and a width of 1. The tension N_x acting on the chord elements is consistent with its tangent direction and forms an included angle α with the coordinate axis *x*. Let *w* be the normal displacement of any point on the membrane surface, which is:

$$N_x \sin\alpha = N_x \tan\alpha = N_x\left(\frac{\partial w}{\partial x}\right)_x$$

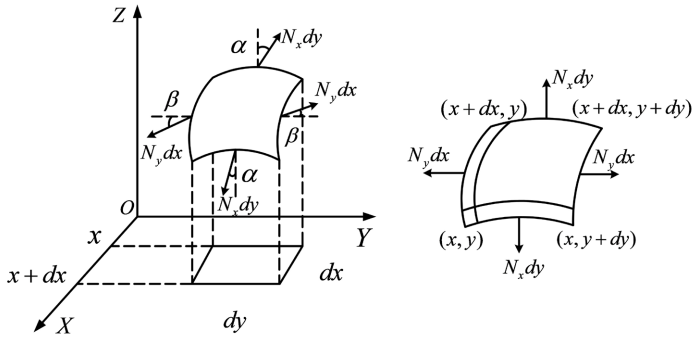

Figure 1. The vibration micro-units of the membrane.

The resultant force in the perpendicular direction acting on the x and $x + \mathrm{d}x$ sides of the element is $N_x\left(\frac{\partial w}{\partial x}\right)_{x+\mathrm{d}x}\mathrm{d}y - N_x\left(\frac{\partial w}{\partial x}\right)_x \mathrm{d}y = N_x\frac{\partial^2 w}{\partial x^2}\mathrm{d}x\mathrm{d}y$

In the same way, the resultant force in the vertical direction on the y and $y + \mathrm{d}y$ edges acting on the surface element is obtained. Let ρ be the surface density of the film material, then the mass of the microsurface element is $\rho\mathrm{d}x\mathrm{d}y$. According to the D'Alembert principle, the equation of motion of the surface element can be obtained as follows:

$$N_x\frac{\partial^2 w}{\partial x^2}\mathrm{d}x\mathrm{d}y + N_y\frac{\partial^2 w}{\partial y^2}\mathrm{d}x\mathrm{d}y = \rho\mathrm{d}x\mathrm{d}y\frac{\partial^2 w}{\partial t^2} + c\mathrm{d}x\mathrm{d}y\frac{\partial w}{\partial t} \tag{9}$$

Equation (9) is simplified to obtain:

$$\rho\frac{\partial^2 w}{\partial t^2} + c\frac{\partial w}{\partial t} - N_x\frac{\partial^2 w}{\partial x^2} - N_y\frac{\partial^2 w}{\partial y^2} = 0 \tag{10}$$

where N_x and N_y are the x-direction (warp direction) and y-direction (weft direction) tension of the membrane surface, respectively; w represents the normal vibration displacement of the membrane, c represents the film damping coefficient.

The membrane material is a flexible material, which is different from the plate and shell structure. Its in-plane stiffness is basically zero. In engineering, the roof membrane material gives the membrane surface a certain stiffness to resist the external load by applying a certain initial pretension. At the same time, the combined effect of wind and rain P is added to the membrane surface. Therefore, the vibration equation of the actual membrane roof can be obtained by adding the initial pretension to the equation of motion (10):

$$\rho\frac{\partial^2 w}{\partial t^2} + c\frac{\partial w}{\partial t} - \left(N_x + N_{0x}\right)\frac{\partial^2 w}{\partial x^2} - \left(N_y + N_{0y}\right)\frac{\partial^2 w}{\partial y^2} = P \tag{11}$$

Define the physical material parameters of the membrane: x-direction pretension N_{0x}; y-direction pretension N_{0y}; Shear force N_{xy}; membrane thickness is h; x-directional Young's modulus of elasticity E_1; Young's modulus of elasticity in y direction E_2; Shear modulus G; x-directional Poisson's ratio μ_1; y-direction Poisson's ratio μ_2, then the governing equations of nonlinear free vibration of orthotropic membrane roof are:

$$\begin{cases} \dfrac{\partial N_x}{\partial x}+\dfrac{\partial N_{yx}}{\partial y}=\dfrac{\partial N_y}{\partial y}+\dfrac{\partial N_{xy}}{\partial x}=0 \\ \rho\dfrac{\partial^2 w}{\partial t^2}+c\dfrac{\partial w}{\partial t}-\left(N_x+N_{0x}\right)\dfrac{\partial^2 w}{\partial x^2}-\left(N_y+N_{0y}\right)\dfrac{\partial^2 w}{\partial y^2}=P \\ \dfrac{1}{E_1 h}\dfrac{\partial^2 N_x}{\partial y^2}-\dfrac{\mu_2}{E_2 h}\dfrac{\partial^2 N_y}{\partial y^2}-\dfrac{\mu_1}{E_1 h}\dfrac{\partial^2 N_x}{\partial x^2}+\dfrac{1}{E_2 h}\dfrac{\partial^2 N_y}{\partial x^2}-\dfrac{1}{Gh}\dfrac{\partial^2 N_{xy}}{\partial x\partial y} \\ =\left(\dfrac{\partial^2 w}{\partial x\partial y}\right)^2-\dfrac{\partial^2 w}{\partial x^2}\dfrac{\partial^2 w}{\partial y^2}-k_{0x}\dfrac{\partial^2 w}{\partial y^2}-k_{0y}\dfrac{\partial^2 w}{\partial x^2} \end{cases} \tag{12}$$

Introducing the stress function $\varphi(x,y)$, then:

$$N_x=h\frac{\partial^2\varphi}{\partial y^2},\quad N_y=h\frac{\partial^2\varphi}{\partial x^2},\quad N_{xy}=-h\frac{\partial^2\varphi}{\partial x\partial y} \tag{13}$$

In the process of membrane vibration, the influence of shear stress is very small. It is approximately considered that $N_{xy}=0$, $N_{0x}=h\sigma_{0x}$, $N_{0y}=h\sigma_{0y}$, then the governing Equations (12) can be simplified as:

$$\begin{aligned} &\rho_0\frac{\partial^2 w}{\partial t^2}+c\frac{\partial w}{\partial t}-\left(h\frac{\partial^2\varphi}{\partial y^2}+N_{0x}\right)\frac{\partial^2 w}{\partial x^2} \\ &-k_{0x}h\frac{\partial^2\varphi}{\partial y^2}-\left(h\frac{\partial^2\varphi}{\partial x^2}+N_{0y}\right)\frac{\partial^2 w}{\partial y^2}=P_W+P_R \end{aligned} \tag{14}$$

$$\frac{1}{E_1}\frac{\partial^4\varphi}{\partial y^4}+\frac{1}{E_2}\frac{\partial^4\varphi}{\partial x^4}=\left(\frac{\partial^2 w}{\partial x\partial y}\right)^2-\frac{\partial^2 w}{\partial x^2}\frac{\partial^2 w}{\partial y^2}-k_{0x}\frac{\partial^2 w}{\partial y^2} \tag{15}$$

The dynamic balance Equation (14) and the deformation coordination Equation (15) together constitute the governing equation of the membrane structure under wind and rain load. Where the displacement and stress boundary conditions are respectively:

$$\begin{cases} w(0,y,t)=0,\dfrac{\partial w}{\partial x}(0,y,t)=0 \\ w(a,y,t)=0,\dfrac{\partial w}{\partial x}(a,y,t)=0 \end{cases},\quad \begin{cases} w(x,0,t)=0,\dfrac{\partial w}{\partial y}(x,0,t)=0 \\ w(x,b,t)=0,\dfrac{\partial w}{\partial y}(x,b,t)=0 \end{cases} \tag{16}$$

$$\begin{cases} \dfrac{\partial^2\varphi}{\partial x^2}(0,y,t)=0 \\ \dfrac{\partial^2\varphi}{\partial x^2}(a,y,t)=0 \end{cases},\quad \begin{cases} \dfrac{\partial^2\varphi}{\partial y^2}(x,0,t)=0 \\ \dfrac{\partial^2\varphi}{\partial y^2}(x,b,t)=0 \end{cases} \tag{17}$$

Assuming that the displacement function satisfying the displacement boundary is:

$$w(x,y,t)=T_{mn}(t)\sin\frac{m\pi x}{a}\sin\frac{n\pi y}{b} \tag{18}$$

Letting $W_{mn}(x,y)=W(x,y)=W$, $T_{mn}(t)=T(t)=T$,

Substituting Equation (18) into Equation (15):

$$\frac{1}{E_1}\frac{\partial^4\varphi}{\partial y^4}+\frac{1}{E_2}\frac{\partial^4\varphi}{\partial x^4}=T^2(t)\frac{m^2n^2\pi^4}{2a^2b^2}\left(\cos\left(\frac{2m\pi x}{a}\right)+\cos\left(\frac{2n\pi y}{b}\right)\right)+T(t)\sin\left(\frac{m\pi x}{a}\right)\sin\left(\frac{n\pi y}{b}\right)k_{0x}\frac{n^2\pi^2}{b^2} \tag{19}$$

Assuming the solution of $\varphi(x,y,t)$ is

$$\varphi(x,y,t)=T^2\left(\alpha\cos\left(\frac{2m\pi x}{a}\right)+\beta\cos\left(\frac{2n\pi y}{b}\right)+\delta_1x^3+\delta_2x^2+\delta_3x+\delta_4y^3+\delta_5y^2+\delta_6y+\delta_7\right)+T(t)\left(\sin\frac{m\pi x}{a}\right)\sin\left(\frac{n\pi y}{b}\right)\xi \tag{20}$$

Letting
$$\begin{cases}\varphi(x,y,t)=T^2(t)\phi_1(x,y)+T(t)\phi_2(x,y)\\ \phi_1(x,y)=\alpha\cos\left(\frac{2m\pi x}{a}\right)+\beta\cos\left(\frac{2n\pi y}{b}\right)+\delta_1x^3+\delta_2x^2+\\ \delta_3x+\delta_4y^3+\delta_5y^2+\delta_6y+\delta_7\\ \phi_2(x,y)=\xi\sin\left(\frac{m\pi x}{a}\right)\sin\left(\frac{n\pi y}{b}\right)=\xi W(x,y)\end{cases}$$

Substituting Equation (20) into Equation (17), we can obtain:

$$\alpha=\frac{E_2n^2a^2}{32m^2b^2},\beta=\frac{E_1m^2b^2}{32n^2a^2}$$

$$\xi=\frac{k_{0x}\left(n\pi/b\right)^2}{\left(\left(n\pi/b\right)^4/E_1\right)+\left(\left(m\pi/a\right)^4/E_2\right)}$$

$$\delta_1=\delta_3=\delta_6=\delta_7=0,\delta_2=\frac{\pi^2E_2n^2}{16b^2},\delta_4=0,\delta_5=\frac{\pi^2E_1m^2}{16a^2}$$

Obviously,

$$\begin{cases}\varphi(x,y,t)=T^2(t)\phi_1(x,y)+T(t)\phi_2(x,y)\\ \phi_1(x,y)=\frac{E_2n^2a^2}{32m^2b^2}\cos\left(\frac{2m\pi x}{a}\right)+\frac{E_1m^2b^2}{32n^2a^2}\cos\left(\frac{2n\pi y}{b}\right)+\frac{\pi^2E_2n^2}{16b^2}x^2+\frac{\pi^2E_1m^2}{16a^2}y^2\\ \phi_2(x,y)=\frac{k_{0x}\left(n\pi/b\right)^2}{\left(\left(n\pi/b\right)^4/E_1\right)+\left(\left(m\pi/a\right)^4/E_2\right)}\sin\left(\frac{m\pi x}{a}\right)\sin\left(\frac{n\pi y}{b}\right)\end{cases} \tag{21}$$

Substituting Equations (18), (20) and (7) into Equation (14), then,

$$\rho_0T''(t)W+cT'(t)W-T(t)\left[k_{0x}h\frac{\partial^2\phi_2}{\partial y^2}+N_{0x}\frac{\partial^2W}{\partial x^2}+N_{0y}\frac{\partial^2W}{\partial y^2}\right]-T^2(t)\left[k_{0x}h\frac{\partial^2\phi_1}{\partial y^2}+h\frac{\partial^2\phi_2}{\partial y^2}\frac{\partial^2W}{\partial x^2}+h\frac{\partial^2\phi_2}{\partial x^2}\frac{\partial^2W}{\partial y^2}\right]-T^3(t)\left[h\frac{\partial^2\phi_1}{\partial y^2}\frac{\partial^2W}{\partial x^2}+h\frac{\partial^2\phi_1}{\partial x^2}\frac{\partial^2W}{\partial y^2}\right]=P_W+P_R \tag{22}$$

The principle of the Galerkin method is that by selecting finite polynomial functions (also called basis functions or shape functions), superimposing them, and then requiring the weighted integral of the results in the solution domain and on

the boundary (the weight function is the trial function itself) to satisfy the original equation, a set of linear algebraic equations that are easy to solve can be obtained, and the natural boundary conditions can be automatically satisfied. Applying the Galerkin method, Equation (22) is transformed into:

$$\begin{aligned}&\iint_s \left\{ \rho_0 T''(t) W + cT'(t) W - T(t) \left(k_{0x} h \frac{\partial^2 \phi_2}{\partial y^2} + N_{0x} \frac{\partial^2 W}{\partial x^2} + N_{0y} \frac{\partial^2 W}{\partial y^2} \right) \right. \\ &-T^2(t) \left(k_{0x} h \frac{\partial^2 \phi_1}{\partial y^2} + h \frac{\partial^2 \phi_2}{\partial y^2} \frac{\partial^2 W}{\partial x^2} + h \frac{\partial^2 \phi_2}{\partial x^2} \frac{\partial^2 W}{\partial y^2} \right) \\ &\left. -T^3(t) \left(h \frac{\partial^2 \phi_1}{\partial y^2} \frac{\partial^2 W}{\partial x^2} + h \frac{\partial^2 \phi_1}{\partial x^2} \frac{\partial^2 W}{\partial y^2} \right) \right\} W(x,y) \mathrm{d}x\mathrm{d}y \\ &= \iint_S (P_W + P_R) W(x,y) \mathrm{d}x\mathrm{d}y\end{aligned} \tag{23}$$

Simplifing the Equation (23), then,

$$AT''(t) + BT'(t) + CT(t) + DT^2(t) + ET^3(t) = P \tag{24}$$

where,

$$A = \iint_s \rho_0 W^2 \mathrm{d}x\mathrm{d}y = \frac{ab}{4} \rho_0$$

$$B = \iint_s cW^2 \mathrm{d}x\mathrm{d}y = \frac{ab}{4} c$$

$$\begin{aligned}C &= \iint_s -\left(k_{0x} h \frac{\partial^2 \phi_2}{\partial y^2} + N_{0x} \frac{\partial^2 W}{\partial x^2} + N_{0y} \frac{\partial^2 W}{\partial y^2} \right) W \mathrm{d}x\mathrm{d}y \\ &= \frac{m^2 \pi^2 b^2 N_{0x} + n^2 \pi^2 a^2 \left(N_{0y} + k_{0x} h \xi \right)}{4ab}\end{aligned}$$

$$D = \iint_s -h \left(k_{0x} \frac{\partial^2 \phi_1}{\partial y^2} + \frac{\partial^2 \phi_2}{\partial y^2} \frac{\partial^2 W}{\partial x^2} + \frac{\partial^2 \phi_2}{\partial x^2} \frac{\partial^2 W}{\partial y^2} \right) W \mathrm{d}x\mathrm{d}y$$

$$E = \iint_s -h \left(\frac{\partial^2 \phi_1}{\partial y^2} \frac{\partial^2 W}{\partial x^2} + \frac{\partial^2 \phi_1}{\partial x^2} \frac{\partial^2 W}{\partial y^2} \right) W \mathrm{d}x\mathrm{d}y = h\pi^4 \frac{3E_1 m^4 b^4 + 3E_2 n^4 a^4}{64 a^3 b^3}$$

$$P = \iint_S (P_W + P_R) W \mathrm{d}x\mathrm{d}y$$

The numerical analytical solution of the tension membrane structure under the coupling action of wind and rain can be obtained by the numerical analytical solution of Equation (24) using Matlab.

4. Validation of Results

In order to verify the correctness of the theoretical derivation in this paper, the experimental results in reference [14] are compared with the analytical solution in this paper. The parameter values are consistent with reference [14]. The surface density of the membrane is 14 kg/cm^2, the thickness is 10 mm, the elastic modulus is 920 Mpa, and the damping coefficient is 86.4 Ns/m. The plane dimension of the membrane structure is 10 m × 10 m. The sagittal-span ratio of the membrane surface is set to two grades, which are 1/10 and 1/12, respectively. The film surface

pretension $N_{0x} = N_{0y}$ is set in two grades: the first grade pretension is 51.1 kN/m and the second grade pretension is 115 kN/m.

Different membrane surface vector-span ratios (1/10 and 1/12), membrane surface pretension grades (grade I pretension and grade II pretension), and wind-driven rain load conditions (I wind I rain, I wind III rain, II wind II rain, III wind I rain, III wind II rain and III wind III rain). Among them, the wind speed range of Class I wind (strong wind) is 17.2 - 20.7 m/s, the wind speed range of Class II wind (strong wind) is 20.8 - 24.4 m/s, and the wind speed range of Class III wind (strong wind) is 24.5 - 28.4 m/s. The rainfall intensity is Class I (64 mm/h), Class II (100 mm/h) and Class III (200 mm/h).

Results are shown in Table 1:

Table 1. Comparison between analytical results and experimental results.

	Vector-span ratio	Pretension	Working condition					
			I wind I rain	I wind III rain	II wind II rain	III wind I rain	III wind II rain	III wind III rain
Analytical results	1/10	I	31.0	36.0	40.0	49.0	50.0	54.0
Experimental results	1/10	I	31.0	36.6	41.4	49.2	50.8	54.4
Relatively poor	-	-	0%	1.6%	3.4%	0.4%	1.6%	0.7%
Analytical results	1/12	I	37.0	42.0	47.0	58.0	60.0	64.0
Experimental results	1/12	I	37.0	43.0	45.0	54.0	60.6	64.2
Relatively poor	-	-	0%	2.3%	4.3%	6.9%	1.0%	0.3%
Analytical results	1/10	II	15.7	18.1	19.9	24.6	25.2	27.0
Experimental results	1/10	II	15.8	18.6	20.2	25.0	25.8	27.6
Relatively poor	-	-	0.6%	2.7%	1.5%	1.6%	4.0%	2.2%
Analytical results	1/12	II	18.6	21.0	24.0	29.0	30.0	32.0
Experimental results	1/12	II	19.2	21.0	24.2	29.6	30.0	32.0
Relatively poor	-	-	3.1%	0%	0.8%	2.0%	0%	0%

The theoretical results are consistent with the experimental results, and the relative difference is less than 10%, which shows that the theoretical method in this paper has good applicability. The theoretical study does not consider the dead weight of membrane material, so the experimental results will be slightly larger than the theoretical results.

5. Conclusions

1) According to the comparative analysis of theoretical results and experimental results, it is concluded that the ratio of membrane surface to span, the grade of membrane surface pretension, the grade of wind speed and rainfall intensity all

have obvious influence on the dynamic response of skeleton supported membrane structure under the coupling action of wind and rain.

2) Although aerodynamic forces will not directly cause instability and damage to the membrane structure, strong nonlinear vibration will occur on the membrane surface when wind and rain loads act together, resulting in the large displacement of the membrane surface. If the load continues to act on the membrane surface, it is very likely that the membrane surface will relax and even cause engineering accidents.

3) The smaller the sagittal-span ratio of the membrane surface, the higher the wind speed grade and rainfall intensity grade, and the greater the displacement of the membrane surface under the coupling action of wind and rain. The greater the pretension of the membrane surface, the smaller the displacement of the membrane surface under the coupling action of wind and rain. Therefore, in the process of designing membrane structure, the ability of the membrane structure to resist external load can be enhanced by improving the membrane surface-span ratio and pretension, so as to ensure that the membrane structure has sufficient structural stability.

Funding

The work is supported by the National Natural Science Foundation of China (Grant No. 51608060).

Conflicts of Interest

The authors declare no conflicts of interest regarding the publication of this paper.

References

[1] Luo, Y.C. (2006) Accident Analysis of Membrane Structure Engineering. *Special Structure*, **23**, 26-29.

[2] Yan, H., Lu, Z.Z. and Wei, G.Q. (2008) Wind Damage Accidents of Membrane Structures and Their Prevention. *Building Structure*, **38**, 113-116.

[3] Xie, L.H. (2015) Two People Were Injured when the Ceiling of Guangzhou Tianhe Olympic Sports Badminton Hall Collapsed. Southern Metropolis Daily, May 4, 2015.

[4] Uematsu, Y., Yamada, M. and Fukushi, M. (1996) Design Wind Load for the Structural Frame of a Long Span Open-Type Roof with Consideration for the Dynamic Response. *Proceedings of Asia-Pacific Conference on Shell and Spatial Structures*, Beijing, 21-25 May 1996, 707-714.

[5] Blocken, B. and Carmeliet, J. (2002) Spatial and Temporal Distribution of Driving Rain on a Low-Rise Building. *Wind and Structures*, **5**, 441-462. https://doi.org/10.12989/was.2002.5.5.441

[6] Sankarana, R. and Paterson, D.A. (1997) Computation of Rain Falling on a Tall Rectangular Building. *Journal of Wind Engineering and Industrial Aerodynamics*, **72**, 127-136. https://doi.org/10.1016/s0167-6105(97)00271-7

[7] Choi, E.C.C. (1993) Simulation of Wind-Driven-Rain around a Building. *Journal of Wind Engineering and Industrial Aerodynamics*, **46**, 721-729. https://doi.org/10.1016/0167-6105(93)90342-l

[8] Li, H.N., Ren, Y.M. and Bai, H.F. (2007) Dynamic Analysis Model of Wind and Rain Excitation of Transmission Tower System. *Chinese Journal of Electrical Engineering*, **27**, 43-48.

[9] Chen, B. (2009) CFD Numerical Simulation of Wind and Rain Pressure on the Surface of Low-Rise Buildings. Harbin Institute of Technology.

[10] Fu, X., Lin, Y.X. and Li, H.N. (2014) Wind Tunnel Test and Response Analysis of High-Voltage Transmission Tower under Combined Action of Wind and Rain. *Engineering Mechanics*, **31**, 72-78.

[11] Wang, H., Li, X.J. and Pan, Z. (2014) Numerical Simulation of Wind-Driven Rain Pressure Loads on Building Facades. *Journal of Civil Engineering*, **47**, 94-100.

[12] Cui, W.H., Zhang, L.M. and Zhang, H.X. (2018) Response Analysis of Saddle-Shaped Membrane Structure under Wind and Rain Action Based on Multiphase Flow Theory. *Industrial Construction*, **48**, 60-64.

[13] Tian, L., Zeng, Y. and Fu, X. (2018) Velocity Ratio of Wind-Driven Rain and Its Application on a Transmission Tower Subjected to Wind and Rain Loads. *Journal of Performance of Constructed Facilities*, **32**, 1-10. https://doi.org/10.1061/(asce)cf.1943-5509.0001210

[14] Li, H.N. and Wang, Q. (2012) Dynamic Response of Point-Supported Glass Curtain Wall with Cable-Truss System under Coupling of Wind and Rain Loads. *Journal of Building Science and Engineering*, **29**, 7-12.

[15] Dong, H., Gao, Q.F. and Deng, Z.W. (2015) Numerical Study on Wind and Rain Load Characteristics of Large Wind Turbines. *Vibration and Shock*, **34**, 17-22.

[16] Gao, Q.F., Dong, H. and Deng, Z.W. (2016) Three-Field Coupling Analysis of Wind and Rain Structure of Large Wind Turbine. *Journal of Central South University* (*Natural Science Edition*), **47**, 1011-1016.

[17] Jiang, S. (2021) Numerical and Experimental Study on the Dynamic Response of Saddle-Shaped Membrane Structure under Wind-Driven Rain Load. Chengdu University of Technology. https://doi.org/10.26986/D.cnki.gcdlc.2021.001360

[18] Pan, R.J., Liu, C.J., Liu, J., *et al.* (2023) Research on Dynamic Response and Reliability of Saddle-Shaped Membrane Structure under Wind-Driven Rain Load. *Vibration and Impact*, **42**, 295-303 +323. https://doi.org/10.13465/j.cnki.jvs.2023.11.035

[19] Xu, Y., Zheng, Z., Liu, C., Song, W. and Long, J. (2011) Aerodynamic Stability Analysis of Geometrically Nonlinear Orthotropic Membrane Structure with Hyperbolic Paraboloid. *Journal of Engineering Mechanics*, **137**, 759-768. https://doi.org/10.1061/(asce)em.1943-7889.0000278

[20] Xu, Y.P., Zheng, Z.L., Liu, C.J., *et al.* (2018) Aerodynamic Stability Analysis of Geometrically Nonlinear Orthotropic Membrane Structure with Hyperbolic Paraboloid in Sag Direction. *Wind and Structures*, **26**, 355-367.